Quantitative proteomics analysis for effect of *Acanthopanax senticosus* extract on Neuroinflammation

Tao Jiang[1], Zhengyang Wang[2], Shenren[3], Ting Xia[1], Xi Zhao[1], Lianhai Jiang[1] and Lirong Teng[1]*

[1]Department of Chemistry and Pharmacy, Zhuhai College of Jilin University, Zhuhai, PR China
[2]Institute of Theoretical Chemistry, Jilin University, Changchun, PR China
[3]College of Traditional Chinese Medicine, Jilin Agricultural University, Changchun, PR China

Abstract: *Acanthopanax senticosus*, a traditional herb commonly found in Northeastern Asia, has been used for treating neurodegenerative diseases. However, the molecular and cellular mechanisms of its effect on neuroinflammation have not been investigated. In the current study, quantitative proteomics approach was applied to investigate the effect of *Acanthopanax senticosus* extract (ASE) on nitrosative stress and inflammatory response in BV-2 microglial cells stimulated with lipopolysaccharide (LPS). The results showed ASE inhibited LPS-induced nitric oxide (NO) production, while no significant toxicity appeared in the cells. Proteomic quantitative analyses using 2D-DIGE (Difference in Gel Electrophoresis) combined with liquid chromatography–electrospray ionization tandem mass spectrometry (LC–ESI-MS/MS) revealed that 17 proteins showed significant changes responding to ASE. Furthermore, signal transduction pathways and network modulated by the ASE were predicted using Ingenuity Pathway Analysis (IPA). These findings indicated the ability of ASE to suppress LPS-induced nitrosative stress in BV-2 cells, and may provide important insights into the molecular mechanism underlying potentially beneficial effect of *Acanthopanax senticosus*.

Keywords: *Acanthopanax senticosus* extract; Microglia; BV-2 cells; 2D-DIGE.

INTRODUCTION

Microglia are erythromyeloid-lineage cells in the central nervous system that are primarily involved in maintenance of the brain and the spinal cord parenchyma tissue homeostasis (Griffiths *et al.*, 2009; Aguzzi *et al.*, 2013; Sugama *et al*., 2009; Bal-Price *et al.*, 2001). They can be activated by bacterial endotoxins such as lipopolysaccharides (LPS) upon phagocytosis of invading bacteria, and produce pro-inflammatory mediators including nitric oxide (NO), which is known to play diverse roles in the regulation of biological processes ranging from development to disease (Moss *et al*., 2001; Streit *et al*., 2005; Saijo *et al*., 2011; Brown *et al*., 2003). There is evidence that excess NO is thought to induce nitrosative stress and contribute to neuronal injuries leading to the progression of neurodegenerative diseases including cerebral ischemia, Parkinson's disease, Alzheimer's disease, Huntington's disease and multiple sclerosis (Sun *et al*., 2010; Glass *et al*., 2010; Liu *et al*., 2013; Tansey *et al*., 2010; Amy *et al*., 2010). Therefore, agents that attentuate chronic microglial activation and suppress production of neurotoxic proinflammatory molecules are of interest for development of novel therapeutic approaches to various neurodegenerative diseases (Aldskogius *et al*., 2001).

With the long history of human civilization, many botanicals possessing antioxidant and antimicrobial properties have been offered beneficial effects on antagonizing inflammatory responses and preventing neurological diseases (Yamagishi *et al*., 2005; Kim *et al*., 2001; Lee *et al*., 2003; Lee *et al*., 2000; Bate *et al*., 2004). As one of the most prominently used traditional medicine used in Northeastern Asia, *Acanthopanax senticosus* has shown its therapeutic effects on diabetes (Zhou *et al*., 2012), ischemia, and ROS production (Chen *et al*., 2002). *In vivo*, ASE was shown to reduce nitric oxide (NO) synthesis by suppressing iNOS expression to attenuate endotoxic shock (Lin *et al*., 2008). These findings suggest that ASE may offer beneficial effects on prevention of neuroinflammation and neurodegenerative diseases. The goal of this study is to investigate the effects of ASE on neuroinflammatory responses in lipopolysaccharide (LPS)-activated murine BV-2 microglial cells using proteomic analysis.

Two dimensional difference in-gel electrophoresis (2D-DIGE) complemented with liquid chromatography tandem mass spectrometry (LC-MS/MS) is a classical proteomic approach, which can visualize and detect differential fold-changes of large numbers of proteins on one gel. It can provide quantitative information, since it minimizes gel-to-gel variation, improves spot matching, reduces number of gels needed, and permits quantitative analysis of small sample amounts (Marouga *et al*., 2005; Calamia *et al*., 2012; Komatsu *et al*., 2006; Sharma *et al*., 2013; Hirano *et al*., 2007). Therefore, such an approach has been mainly applied in discovering novel biomarkers and understanding the molecular mechanisms of action of specific molecules.

**Corresponding author:* e-mail: tenglr@jlu.edu.cn

In the present study, We examined the effect of ASE on LPS-stimulated microglial BV2 cells. Using 2D-DIGE in couple with liquid chromatography tandem mass spectrometry (LC-MS/MS), we identified multiple molecular targets of ASE in LPS-stimulated BV-2 cells. Furthermore, we predicted signal transduction pathways and protein network that are modulated by ASE using Ingenuity Pathway Analysis (IPA). These findings indicated the ability of ASE to attenuate LPS-induced nitrosative stress in BV-2 cells and may provide important insights into the molecular events underlying the treatment of ASE and allow the identification of novel therapeutic targets.

EXPERIMENTAL

Materials

ASE were purchased from Xi'an Acetar Biology and Technology Co., Ltd. (Xi'an, China). Dulbecco's modified Eagle's cell culture medium (DMEM) was obtained from Gibco (Invitrogen Co., San Diego, CA, USA). Sequencing-grade trypsin was obtained from Promega (Madison, WI, USA). Fetal bovine serum (FBS) was obtained from Hangzhou Sijiqing Company (Hangzhou, China). Lipopolysaccharide (LPS) (rough strains) from Escherichia coli F583 (Rd mutant), N-omega-Nitro-L-Arginine Methyl Ester Hydrochloride (L-NAME) and methylthiazolyldiphenyl-tetrazolium bromide (MTT) were from Sigma-Aldrich (St. Louis, MO). CyDye DIGE Fluor minimal dyes and DryStrip gels (24 cm, pH 3-10) were purchased from GE Healthcare (Buckinghamshire, UK).

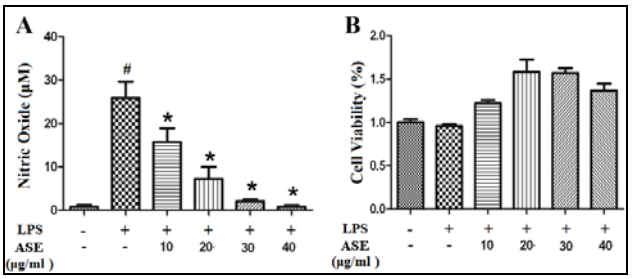

Fig. 1: Dose titration for administration of ASE. BV-2 cells were treated with LPS in the presence of 0, 10, 20, 30, or 40μg/mL ASE for 16 hours. (A) A Griess assay showed NO level significantly increased after LPS-exposure (*, $p<0.05$ vs. untreated), but inhibited by ASE in a dose-dependent manner (#, $p<0.05$ vs. LPS-treated by one-way ANOVA, n=3; data present as mean ± SEM). (B) Result of MTT assay indicated the addition of ASE did not significantly affect the cell viability.

Cell culture and treatment

Murine microgial BV-2 cells were cultured with Dulbecco's Modified Eagle Medium (DMEM) supplemented with 10% FBS containing 100 units/mL penicillin and 100 μg/mL streptomycin, and maintained in 5% CO2 incubator at 37°C. At 70-80% confluence, cells were starved in DMEM without FBS for 3 hours. Then, the cells were exposed to 100ng/mL LPS for 16 hours in the presence or absence of ASE, which was added to the culture medium 1 hour prior to LPS exposure. 0.5mM L-NAME was added to the medium 1 hour prior to LPS exposure as a positive control.

Assessing cell viability

A MTT assay was performed to access cell viability. Cells were treated with specified concentrations of ASE. Then, the conditioned medium was removed and 100μL of MTT reagent (0.5mg/mL) dissolved in DMEM was added to each well. The plates were incubated for 3 h at 37°C. The formazan particles were dissolved with 100μL DMSO, and absorbance was measured at 540 nm using a microplate reader (Biotek Synergy 2, Winooski, VT).

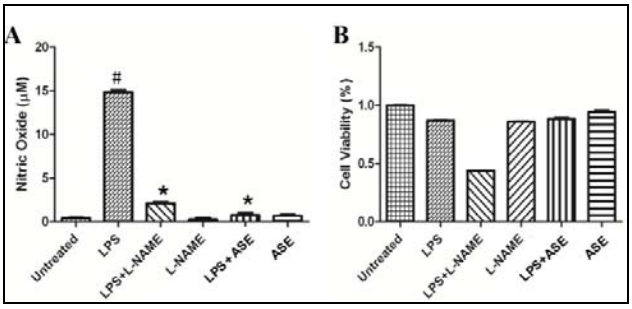

Fig. 2: Effects of ASE on neuroinflammatory response induced by LPS in BV-2 cells. (A) Griess assays showed that NO productions in BV-2 cells induced by LPS were significantly inhibited by 20μg/mL ASE as well as 0.5 mM L-NAME. #, $p<0.05$ vs. untreated; *, $p<0.05$, vs. LPS-treated by one-way ANOVA, n=3; Data present as mean ± SEM. The ASE or L-NAME alone has no significantly effect on NO production or cytotoxicity. (B) Results of MTT assay indicated under such conditions, LPS exposure resulted in minor cell death.

Nitric Oxide (NO) determination

After cell treatment for 16 hours, aliquots of conditioned medium (50μL) was collected to incubate with 50μL of Griess reagent (1% (w/v) sulfanilamide and 0.1% (w/v) N-(1-naphthyl) ethylenediamide in 5% (v/v) phosphoric acid) for 10 min at room temperature covered in dark. Absorbance was measured at 543 nm using the BioTek Synergy 2 micro-plate reader and NO concentration was determined from a standard curve of sodium nitrite dilution series.

Protein extraction

The cell samples from the control and experimental groups were frozen in liquid nitrogen and then crushed by using a mortar and pestle. All samples were lysed with a lysis buffer containing 7M urea, 2M thiourea, 4% w/v CHAPS and 30mM Tris, pH 8.5. All samples were centrifuged at 15,000×g for 15 min at 4°C and the supernatant was collected. Protein concentration was determined with the BCA protein assay kit following the

manufacturer's instructions. The samples were then aliquoted and stored at -80 °C for further analysis.

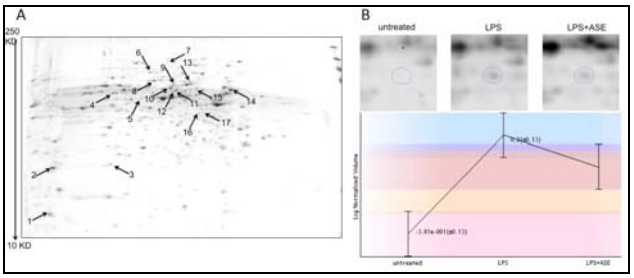

Fig. 3: Progenesis SameSpot analysis of the 2-D DIGE results. A total of 17 spots were found occurring significant protein level changes between LPS-treated and LPS+ASE-treated samples ($p<0.05$, fold change >1.5) (A) A representative 2-D DIGE gel showing the differentially expressed spots. (B) An example spot of down-regulated by ASE (Spot #13, p = 1.263e-004, fold change = 2.0).

Labeling proteins with CyDye

Labeling of proteins for 2D-DIGE was performed according to manufacturer's protocol (ratio of 50µg protein to 400 pmol CyDye™ dyes). To ensure that there were no dye-specific labeling artifacts, sample replicates in different gels were labeled with either Cy3 or Cy5 dye, whereas the pooled internal reference sample, a mixture of same amounts of all analyzed samples, was labeled with Cy2 dye.

Two-dimensional electrophoresis

The labeled protein samples were pooled and brought up to a final volume of 420µL with rehydration buffer (8 M urea, 4% CHAPS, 2% IPG buffer , pH range 3-10, 20 mM dithiothreitol (DTT). The first-dimension isoelectric focusing (IEF) was performed in an IPGphor IEF unit on 24-cm IPG strips pH 3-10. After IEF, the proteins were reduced and alkylated by successive 15 minutes treatments with equilibration buffer containing 1.0% (w/v) DTT, followed by 2.5% (w/v) iodoacetamide. Proteins on the strips were further resolved by 12% SDS-PAGE. All gels were run at 1 Watt/gel in the dark overnight.

Gel image acquisition and DIGE data analysis

The gel images were acquired on an Ettan DIGE imager scanner. Excitation and emission wavelengths were set specifically for each dye according to the manufacturer's recommendations. After imaging for CyDyes, The gels were stained by the Coomassie stainning method. DIGE data was processed by SameSpots software (Version 4.5; Totallab Nonlinear USA Inc. Durham, North Carolina) (Karp *et al*., 2008).

Protein preparation for LC-MS/MS

Protein spots of interest were manually excised from stained gels and digested by the enzyme solution containing sequencing-grade modified porcine trypsin for 16 h at 37°C. The peptides were desalted by using ZipTip C18 pipette tips (Millipore, Bedford, MA, USA). Full-scan MS and MS/MS experiments were carried out with Thermo Scientific LTQ™ Orbitrap-XL in positive ion reflector mode. Approximately 4µL of sample was loaded and the peptides were separated and eluted from the analytical column with a gradient of acetonitrile from a 10% to 60% for 100 min at 250nL/minute. The Sorcerer 2IDA (Sage-N research Inc., San Jose, California) was used to query the data against the IPI-mouse database. Raw data were copied to the sorcerer and searched against the database.

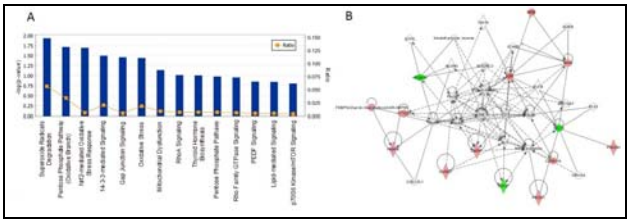

Fig. 4: Effect of ASE in LPS-induced microglial BV-2 cells on canonical pathways and signaling network. (A) Top 14 canonical pathways participated by the differentially expressed proteins responding to ASE treatment in BV-2 cells. (B) The top protein network responding to ASE treatment in BV-2 cells. The symbols labeled in red and green represent up-and down-regulation, respectively and the intensity of the colors indicate the degree of regulation. Solid lines in the network imply direct interactions between proteins, and dashed lines indicate indirect interactions.

STATISTICAL ANALYSIS

Data shown represent the mean and standard error. Statistical analysis was performed with one-way analysis of variance (ANOVA). Data were considered statistically significant at $p < 0.05$.

Bioinformatic analysis

The identified proteins were uploaded into the Ingenuity Pathway Analysis (IPA) software version 7.6. Canonical pathways and protein-protein network were predicted using IPA (Kramer *et al*., 2014).

RESULTS

The effect of ASE on cells viability and NO production in LPS-stimulated BV2 cells

To determine the effect of ASE in LPS-simulated BV-2 cells, we first conducted dose titrations for ASE. BV-2 cells were treated with various concentration of ASE (0, 10, 20, 30, 40µg/mL) in the presence of LPS. A Griess assay showed that NO level significantly increased by LPS induction compared with the untreated control (fig. 1A). Whereas administration of ASE decreased NO production and more inhibitions were seen as the

Table 1: List of the differentially expressed proteins identified by LC-MS/MS analysis

Spot	Protein name	Protein accession numbers	Symbol	Molecular weight (Da)	Fold Change	Sequence coverage
1	Ubiquitin-like protein ISG15	IPI00555085	ISG15	17,897.50	-1.9	56.2%
2	Peroxiredoxin-1	IPI00121788	PRDX1	22,177.50	1.6	84.4%
3	Superoxide dismutase [Mn], mitochondrial	IPI00109109	SOD2	24,603.20	-1.7	50.6%
4	Immune-responsive gene 1 protein	IPI00111285	IRG1	53,759.60	1.6	69.8%
5	Cathepsin D	IPI00111013	CTSD	44,955.00	1.5	57.4%
6	Moesin	IPI00110588	MSN	67,768.80	1.6	80.1%
7	Ezrin	IPI00330862	EZR	69,408.80	2.1	56.9%
8	EH domain-containing protein 1	IPI00126083	EHD1	60,605.20	1.53	80.8%
9	Glucose-6-phosphate 1-dehydrogenase X	IPI00228385	G6PD	59,263.60	1.6	77.90%
10	D-3-phosphoglycerate dehydrogenase	IPI00225961	PHGDH	56,585.20	1.5	54.60%
11	Coronin-1A	IPI00323600	CORO1A	50,988.90	1.6	53.40%
12	UMP-CMP kinase 2, mitochondrial	IPI00120113	CMPK2	50,036.40	-1.9	73.20%
13	Protein disulfide-isomerase A3	IPI00230108	PDIA3	56,680.40	-2.0	74.90%
14	Tubulin alpha-1C chain	IPI00403810	TUBA1C	49,909.60	1.8	58.10%
15	Peptidyl-prolyl cis-trans isomerase FKBP4	IPI00230139	FKBP4	51,573.10	1.5	76.00%
16	Glutaredoxin-3	IPI00315550	GLRX3	37,778.70	1.5	53.40%
17	26S proteasome non-ATPase regulatory subunit 13	IPI00126048	PSMD13	42,810.00	1.6	61.70%

concentrations of ASE increased. MTT assay result indicated no significant cell death was caused by addition of ASE (fig. 1B). ASE treatment alone had neither cytotoxicity to the cells nor showed any significant effects on NO production (fig. 2). As a positive control, treatment with a known NO inhibitor L-NAME ensured the inhibitory response to the LPS-stimulated BV-2 cells. Following these findings, we chose to use 20μg/mL concentrations for the next set of 2D-DIGE experiments designated to identify molecular targets of ASE in LPS-stimulated BV2 cells.

Modulation of ASE on protein expression in LPS-stimulated microglial BV-2 Cells

To determine the global proteomic changes after ASE treatment in LPS-stimulated BV-2 cells, we next performed 2D-DIGE followed by LC-MS/MS analysis. Three samples (untreated, LPS-treated, treated with LPS + ASE) in biological triplicates were lysed and labeled by CyDyes. After 2D-DIGE separation, images of the gels were subjected to quantitative analysis using the SameSpots software. A total of 935 protein spots were detected, of which 17 spots were significantly altered (fold change > 1.5, $p<0.05$) by the treatments. These spots were depicted on a representative DIGE gel image shown in fig. 3A. Representative quantification of spot #13 (fig. 3B) were presented as an examples of down-regulation in the LPS + ASE treatment group. Next, the 17 differential spots were excised on the corresponding Coomassie staining gel for protein identification by LC-MS/MS. The identified proteins are listed in table 1.

DISCUSSION

In order to get more insight on the mechanisms for the action of ASE under LPS-induced microglial activation, we predicted canonical pathways and protein-protein interaction network affected by ASE in LPS-stimulated BV-2 cells using IPA data on differentially expressed proteins. The top canonical pathways revealed the proteins altered by ASE are mainly involved in superoxide radicals degradation, pentose phosphate pathway (oxidative branch), nrf2-mediated oxidative stress response, 14-3-3-mediated signaling, and gap junction signaling (fig. 5). Protein-protein interaction network, which is associated with ASE treatment, were further examined by IPA analysis. The results showed that 14 out of the 17 proteins are involved in this network. Among these proteins, 3 proteins are down-regulated (shaded green) and 11 proteins are up-regulated (shaded red). They mainly play roles in cell death and survival, protein synthesis and free radical scavenging. These results indicated that ASE treatment can significantly decrease neuroinflammation by regulating expression of many proteins that are involved in multiple oxidative stress-related pathway, consistent with their known antioxidant effects.

CONCLUSIONS

In the present study, we applied quantitative proteomics to investigate the effect of ASE in LPS-induced BV-2 cells. Our findings provide detailed mechanistic insights

into the multiple protein targets of ASE. Moreover, based on the expression levels of the differentially expressed proteins, we predicted the signal transduction pathways and network associated with these proteins. These studies provide molecular evidence for the underlying mechanism of their multi-modal action of ASE and may aid in better understanding of the molecular mechanisms of its preventive effect against neurological diseases.

ACKNOWLEDGEMENTS

The authors would like to thank the National Natural Science Foundation of China (No.81403077).

REFERENCES

Aguzzi A, Barres BA and Bennett ML (2013). Microglia: Scapegoat saboteur or something else? *Science,* **339**: 156-161.

Aldskogius H (2001). Regulation of microglia-potential new drug targets in the CNS. *Expert Opin Ther Targets,* **5**: 655-668.

Amy HM, Matthew JB, Grace EB, Colin MW, Hilary MR, Christopher JS, James LM and Amanda KH (2010). Non-steroidal Anti-inflammatory drugs in alzheimer's disease and parkinson's disease: Reconsidering the role of neuroinflammation. *Pharmaceuticals* (Basel), **3**: 1812-1841.

Bal-Price A and Brown GC (2001). Inflammatory neurodegeneration mediated by nitric oxide from activated glia-inhibiting neuronal respiration, causing glutamate release and excitotoxicity. *J Neurosci.,* **21**: 6480-6491.

Bate C, Salmona M and Williams A (2004). Ginkgolide B inhibits the neurotoxicity of prions or amyloid-beta1-42. *J. Neuroinflammation,* **1**: 4.

Brown GC and Bal-Price A (2003). Inflammatory neurodegeneration mediated by nitric oxide, glutamate, and mitochondria. *Mol. Neurobiol.,* **27**: 325-355.

Calamia V, Fernandez-Puente P, Mateos J, Lourido L, Rocha B, Montell E, Verges J, Ruiz-Romero C and Blanco FJ (2012). Pharmacoproteomic study of three different chondroitin sulfate compounds on intracellular and extra cellular human chondrocyte proteomes. *Mol. Cell Proteomics,* **11**: 1-14.

Chen ML, Song FR, Guo MQ, Liu ZQ and Liu SY (2002). Analysis of flavonoid constituents from leaves of Acanthopanax senticosus Harms by electrospray tandem mass spectrometry. *Rapid Commun. Mass Spectrom,* **16**: 264-271.

Glass CK, Saijo K, Winner B, Marchetto MC and Gage FH (2010). Mechanisms underlying inflammation in neurodegeneration. *Cell,* **140**: 918-934.

Griffiths MR, Gasque P and Neal JW (2009). The multiple roles of the innate immune system in the regulation of apoptosis and inflammation in the brain. *J. Neuropathol. Exp. Neurol.,* **68**: 217-226.

Hirano M, Rakwal R, Kouyama N, Katayama Y, Hayashi M, Shibato J, Ogawa Y, Yoshida Y, Iwahashi H and Masuo Y (2007). Gel-based proteomics of unilateral irradiated striatum after gamma knife surgery. *J. Proteome Res.,* **6**: 2656-2668.

Karp NA, Feret R, Rubtsov DV and Lilley KS (2008). Comparison of DIGE and post-stained gel electrophoresis with both traditional and same spots analysis for quantitative proteomics. *Proteomics,* **8**: 948-960.

Kim H, Kim YS, Kim SY and Suk K (2001). The plant flavonoid wogonin suppresses death of activated C6 rat glial cells by inhibiting nitric oxide production. *Neurosci. Lett.,* **309**: 67-71.

Komatsu S, Zang X and Tanaka N (2006). Comparison of two proteomics techniques used to identify proteins regulated by gibberellin in rice. *J. Proteome Res.,* **5**: 270-276.

Kramer A, Green J, Pollard J Jr and Tugendreich S (2014). Causal analysis approaches in Ingenuity Pathway Analysis. *Bioinformatics,* **30**: 523-530.

Lee H, Kim YO, Kim H, Kim SY, Noh HS, Kang SS, Cho GJ, Choi WS and Suk K (2003). Flavonoid wogonin from medicinal herb is neuroprotective by inhibiting inflammatory activation of microglia. *FASEB J.,* **17**: 1943-1944.

Lee S, Suh S and Kim S (2000). Protective effects of the green tea polyphenol (-)-epigallocatechin gallate against hippocampal neuronal damage after transient global ischemia in gerbils. *Neurosci. Lett.,* **287**: 191-194.

Lin QY, Jin LJ, Cao ZH, Li HQ and Xu YP (2008). Protective effect of *Acanthopanax senticosus* extract against endotoxic shock in mice. *J. Ethnopharmacol.,* **118**: 495-502.

Liu GY, Li XD, Wang TT, Zhou Z and Song JM (2013). The relationship between the expression of CIDE-B and the neuronal apoptosis following cerebral ischemia reperfusion in rats. *Int. J. Pharmacol.,* **9**: 379-384.

Marouga R, David S and Hawkins E (2005). The development of the DIGE system: 2D fluorescence difference gel analysis technology. *Anal. Bioanal. Chem.,* **382**: 669-678.

Moss DW and Bates TE (2001). Activation of murine microglial cell lines by lipopolysaccharide and interferon-gamma causes NO-mediated decreases in mitochondrial and cellular function. *Eur. J. Neurosci.,* **13**: 529-538.

Saijo K and Glass CK (2011). Microglial cell origin and phenotypes in health and disease. *Nat. Rev. Immunol.,* **11**: 775-787.

Sharma NK, Sethy NK and Bhargava K (2013). Comparative proteome analysis reveals differential regulation of glycolytic and antioxidant enzymes in cortex and hippocampus exposed to short-term hypobaric hypoxia. *J. Proteomics,* **79**: 277-298.

Streit WJ, Conde JR, Fendrick SE, Flanary BE and Mariani CL (2005). Role of microglia in the central nervous system's immune response. *Neurol. Res.,* **27**: 685-691.

Sugama S, Takenouchi T, Cho BP, Joh TH, Hashimoto M and Kitani H (2009). Possible roles of microglial cells for neurotoxicity in clinical neurodegenerative diseases and experimental animal models. *Inflamm. Allergy Drug Targets,* **8**: 277-284.

Sun GY and Wood WG (2010). Recent developments in understanding oxidative mechanisms and contributions of glial cell activation, mitochondrial dysfunction and lipids and signaling pathways to neurodegenerative diseases. *Preface Mol. Neurobiol.,* **41**: 53-54.

Tansey MG1 and Goldberg MS (2010). Neuro-inflammation in Parkinson's disease: Its role in neuronal death and implications for therapeutic intervention. *Neurobiol. Dis.,* **37**: 510-518.

Yamagishi S, Nakamura K, Jinnouchi Y, Takenaka K and Imaizumi T (2005). Therapeutic implications of blockers of advanced glycation end products (AGEs)-their receptor (RAGE) system. *Int. J. Pharmacol.,* **1**: 203-209.

Zhou H, Xing JP, Liu S, Song FR, Cai ZW, Pi ZF, Liu ZQ and Liu SY (2011). Screening and determination for potential alpha-glucosidase inhibitors from leaves of *Acanthopanax senticosu*s harms by using UF-LC/MS and ESI-MS (n). *Phytochem. Anal.,* **23**: 315-323.